2010 JINST 5 P05005

Relative luminosity measurement of the LHC with the ATLAS forward calorimeter

The HiLum ATLAS Endcap collaboration

A. Afonin,[h] **A.V. Akimov,**[e] **T. Barillari,**[f] **V. Bezzubov,**[h] **M. Blagov,**[e] **H.M. Braun,**[k]
D. Bruncko,[c] **S.V. Chekulaev,**[j] **A. Cheplakov,**[b] **R. Degele,**[d] **S.P. Denisov,**[h] **V. Drobin,**[b]
P. Eckstein,[a] **V. Ershov,**[b] **V.N. Evdokimov,**[h] **J. Ferencei,**[c] **V. Fimushkin,**[b] **A. Fischer,**[f]
H. Futterschneider,[a] **V. Garkusha,**[h] **A. Glatte,**[a] **C. Handel,**[d] **J. Huber,**[f] **N. Javadov,**[b]
M. Kazarinov,[b] **A. Khoroshilov,**[g] **A.E. Kiryunin,**[f] **E. Kladiva,**[c] **M. Kobel,**[a] **A.A. Komar,**[e]
M. Komogorov,[b] **A. Kozelov,**[h] **G. Krupny,**[h] **V. Kukhtin,**[b] **S. Kulikov,**[h]
L.L. Kurchaninov,[j] **E. Ladygin,**[b] **A.B. Lazarev,**[b] **A. Levin,**[h] **W.F. Mader,**[a]
A.L. Maslennikov,[g] **S. Menke,**[f] **L. Merkulov,**[b] **A. Neganov,**[b] **H. Oberlack,**[f] **C.J. Oram,**[j]
R. Othegraven,[d] **S.V. Peleganchuk,**[g] **V. Petrov,**[b] **S. Pivovarov,**[g] **G.E. Pospelov,**[f]
N. Prokopenko,[h] **J. Rascvetalov,**[h] **N.Rusakovich,**[b] **J.P. Rutherfoord,**[i] **D. Salihagic,**[f]
A.Y. Savine,[i] **P. Schacht,**[f] **H. Secker,**[d] **F. Seifert,**[a,1] **V. Seleznev,**[h] **L. Shaver,**[i]
S. Shilov,[b] **A.A. Snesarev,**[e] **M. Soldatov,**[h] **J. Spalek,**[c] **M. Speransky,**[e] **D. Stoyanova,**[h]
A. Straessner,[a] **P. Strizenec,**[c] **V.V. Sulin,**[e] **A. Talyshev,**[g] **S. Tapprogge,**[d]
Yu.A. Tikhonov,[g] **Y. Usov,**[b] **V. Vadeev,**[b] **I. Vasiliev,**[h] **R. Walker**[i] **and C. Zeitnitz**[k]

[a]*Technische Universität Dresden, Dresden, Germany*

[b]*Joint Institute for Nuclear Research, Dubna, Russia*

[c]*Institute of Experimental Physics of the Slovak Academy of Sciences, Kosice, Slovakia*

[d]*University of Mainz, Mainz, Germany*

[e]*LPI, Lebedev Physical Institute, Moscow, Russia*

[f]*Max-Planck-Institut für Physik, Munich, Germany*

[g]*BINP, Budker Institute of Nuclear Physics, Novosibirsk, Russia*

[h]*IHEP, Institute for High Energy Physics, Protvino, Russia*

[i]*University of Arizona, Tucson, U.S.A.*

[j]*TRIUMF, Vancouver, Canada*

[k]*University of Wuppertal, Wuppertal, Germany*

E-mail: Frank.Seifert@cern.ch

[1]Corresponding author.

ABSTRACT: In this paper it is shown that a measurement of the relative luminosity changes at the LHC may be obtained by analysing the currents drawn from the high voltage power supplies of the electromagnetic section of the forward calorimeter of the ATLAS detector. The method was verified with a reproduction of a small section of the ATLAS forward calorimeter using proton beams of known beam energies and variable intensities at the U-70 accelerator at IHEP in Protvino, Russia. The experimental setup and the data taking during a test beam run in April 2008 are described in detail. A comparison of the measured high voltage currents with reference measurements from beam intensity monitors shows a linear dependence on the beam intensity. The non-linearities are measured to be less than 0.5 % combining statistical and systematic uncertainties.

Contents

1 Introduction

ATLAS [1] is a multi-purpose physics detector at the Large Hadron Collider (LHC) [2] at CERN. It records the products of proton-proton collisions at centre-of-mass energies up to 14 TeV. The instantaneous luminosity of the LHC is planned to be 10^{34} cm^{-2} s^{-1}. For many of the anticipated physics analyses, in particular for measurements of absolute cross-sections, the knowledge of the integrated luminosity is essential. It will be provided by the luminosity detectors LUCID [1, 3], used for a relative luminosity measurement, and ALFA [3, 4], used for an absolute calibration of the luminosity determination at low instantaneous luminosities of about 10^{27} cm^{-2} s^{-1}. For the absolute calibration, a precision of about 3% is aspired [3]. For the relative measurement using LUCID, a statistical uncertainty of about 1% is expected after 3 minutes of recording time [5]. The information about relative changes in luminosity are also important for monitoring beam stability and beam degradation in order to efficiently operate the ATLAS trigger and data acquisition system.

Here, we discuss an alternative method to obtain a continuous measurement of the relative change in instantaneous luminosity at the LHC using the currents drawn from the high voltage (HV) power supplies in the electromagnetic section of the ATLAS liquid-argon forward calorimeter, FCal1 [1, 6].

It is based on the measurement of the currents induced by ionisation of the liquid argon (LAr) by particles produced in proton-proton collisions. The dominant physics process at the LHC is

inelastic proton-proton scattering, with a cross-section of about 80 mb [7, 8]. For each bunch crossing an average of 23 inelastic events [7] will be produced at nominal LHC luminosity. They deposit most of their energy in the forward section of the detector. The ionisation and thus the HV currents are expected to scale linearly with the instantaneous luminosity up to the nominal LHC luminosity. While LUCID can in principle provide a measurement for every proton bunch, the method presented here is limited by the HV current readout cycle time of several seconds. Therefore only a determination averaged over many bunch-crossings will be possible with this method. The feasibility of this method is verified in a test beam at the U-70 proton accelerator [9] in Protvino, Russia, using a test module of the FCal1. Possible non-linearities could be caused by a reduction of the HV at high currents or positive ion build-up in the gaps [10].

This paper is organised as follows: In section 2 the beam parameters and beam structure of the U-70 accelerator in Protvino are described, as well as the experimental setup and the beam monitoring. Furthermore, the test module of the FCal1 and the readout of the currents drawn from the HV power supplies are described. Section 3 discusses the analysis of the data. A summary and conclusion are given in section 4.

2 Test beam configuration

2.1 Purpose of the test beam run

The aim of the HiLum project [11–13] is the study of the behaviour of the electromagnetic endcap calorimeter, EMEC [1], the hadronic endcap calorimeter, HEC [1], and the electromagnetic section of the forward calorimeter, FCal1, in the environment of high particle rates expected for the LHC upgrade phase (sLHC) [14]. At the sLHC instantaneous luminosities of up to 10^{35} cm^{-2} s^{-1} are foreseen. The high interaction rate and particle flux in the test beam were obtained by placing small calorimeter test modules directly into the Protvino accelerator proton beam behind iron absorbers. The layout and material of these modules are similar to that used in the ATLAS detector. Different LHC luminosities have been simulated experimentally by varying the beam intensities at a constant beam energy of 60 GeV using the bent crystal technique [15] for beam extraction. The expected energy flux through the calorimeters was calculated to correspond to operating conditions in ATLAS and the test beam setup was optimised accordingly by Monte-Carlo simulations [11].

During the test beam periods the U-70 was filled with five bunches of protons (p) separated by a gap of about 990 ns. Each bunch was of 166 ns length, but only about 30 ns were occupied by protons. One accelerator fill was extracted over a time interval of about 1.2 s, henceforth referred to as 'spill length'. The spill cycle time was about 9.5 s leading to a gap of about 8.3 s between two spills. Beam intensities were ranging from 10^7 p/spill to 10^{12} p/spill after extraction.

2.2 Experimental setup and beam monitoring

The experimental setup used at the high luminosity beam line in Protvino is shown in figure 1. Several beam monitoring devices were installed between the extraction point and the calorimeter cryostats. An evacuated secondary emission chamber containing a matrix of 5 mm wide electrode strips was used for beam position measurements in the high intensity range. An ionisation chamber provided accurate measurements of the integrated beam intensity per spill up to 10^{11} p/spill. Its absolute calibration was done using activated aluminium foils. A scintillation counter hodoscope for
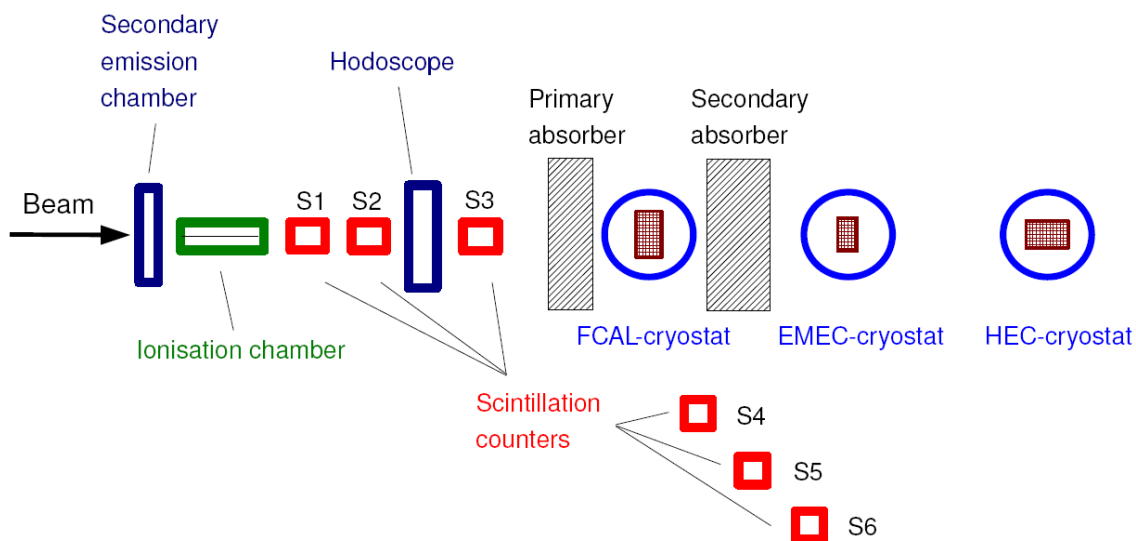
Figure 1. Schematic layout of the experimental setup of the high luminosity test beam. The beam direction is from left to right. See text for details.

beam profile measurements and six scintillation counters, three in the beam line (S1-S3) and three at large angles (S4-S6) with respect to the beam, were also installed. They were used as a cross-check for the ionisation chamber measurements and served as a bunch trigger as well. The hodoscope and the counters S1, S2, and S3 were operational only at low intensities up to $5 \cdot 10^7$ p/spill and had to be moved out of the beam at higher intensities to avoid damage. The counters S4, S5, and S6 were detecting secondary particles from beam interactions with the absorber material and could therefore be used during high intensities.

2.3 The FCALchick and the readout of the HV currents

The FCal1 in ATLAS consists of a copper absorber matrix in which a hexagonal array of concentric copper tubes (anodes) and copper rods (cathodes) with 250 μm wide liquid-argon gaps between is embedded [1, 16]. The prototype of the FCal1 used in Protvino, referred to as the FCALchick, consisted of one section of 16 electrodes with 250 μm LAr gaps and one section of 16 electrodes with 100 μm LAr gaps, a prototype of the design being proposed for the sLHC. The electrodes of the FCALchick are only 50 mm long compared to 450 mm [1, 16] in the ATLAS FCal1. An additional liquid-nitrogen loop is included for extra cooling. The layout and a picture of the FCALchick are shown in figure 2. The shaded circles indicate the beam size in front of the absorbers. Groups of four electrodes were connected in parallel. The eight groups of the FCALchick were connected to a signal readout wire and a high voltage supply wire. The low pass filter for each HV channel had resistors of 10 kΩ and filter capacitors of 220 nF, corresponding to a time constant of 2.2 ms.

The expected HV currents drawn by the FCALchick readout channels for different beam intensities are shown in table 1, together with the corresponding LHC luminosities. The comparison to the various luminosities in ATLAS which gives the same HV current density as observed in the FCalchick is obtained by using the GEANT4 [17] simulation code of this test beam setup along
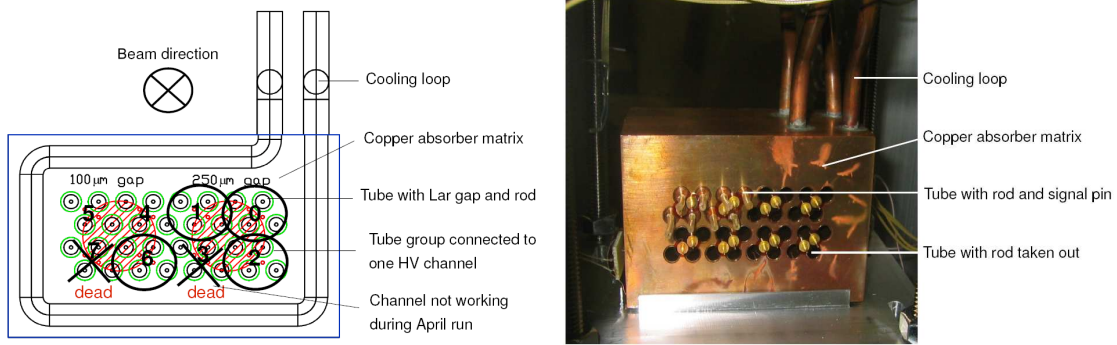
Figure 2. Left: Channel layout during the April 2008 data taking run. Channels surrounded by circles were connected to the additional measurement device. Channels crossed out were not operational during the April run. Right: The FCALchick used in the Protvino test beams. The copper absorber matrix holds the rods with signal pins. Some of the rods are not installed. Also visible is the cooling loop for liquid-nitrogen cooling.

Table 1. Beam intensities and FCALchick (250 μm side) HV currents estimated before the test beam run for the various beam intensities. The parameters are extrapolated linearly to the highest intensities.

Protons/spill	10^7	10^8	10^9	10^{10}	10^{11}	10^{12}
Protons/bunch	5	50	500	5000	$5 \cdot 10^4$	$5 \cdot 10^5$
LHC luminosity equivalent [cm^{-2} s^{-1}]	10^{32}	10^{33}	10^{34}	10^{35}	10^{36}	10^{37}
HV current / channel [μA]	0.12	1.2	12	120	1200	12000

with GEANT4 simulations of minimum bias proton-proton collisions in the ATLAS detector. Both simulations give the rate of ionisation in the 250 μm FCal-style gaps. For the ATLAS simulation comparisons, gaps near the highest pseudorapidity covered by the forward calorimeter were chosen at a depth in the calorimeter near the electromagnetic shower maximum.

In the test beam setup an ISEG [18] HV supply module with effective 16 bit analog-to-digital converters (ADC) for internal HV current measurement was installed, leading to a resolution of about 200 nA over a range of ±10 mA. The readout cycle time was 1 s. This was estimated to be insufficient for the proposed measurements, especially considering the expected HV currents in the low intensity region (compare table 1).

To improve the precision, an external measurement device for the HV current with 24 bit ADCs and a resolution of 1.2 nA per bit was used. The logging rate of the device was at 10 Hz per channel and the precision of the time-stamp was 10 ms. Electronic noise mainly from the HV power supply limited the effective resolution to about 25 nA, depending on the channel. A picture of the measurement device is shown in figure 3. The data transfer and independent power supply of the measurement device was realised by a LAN-cable connecting it to a data acquisition PC. In ATLAS, the HV power supplies use 20 bit ADCs for internal HV current readout providing a sufficient precision without an external ammeter.
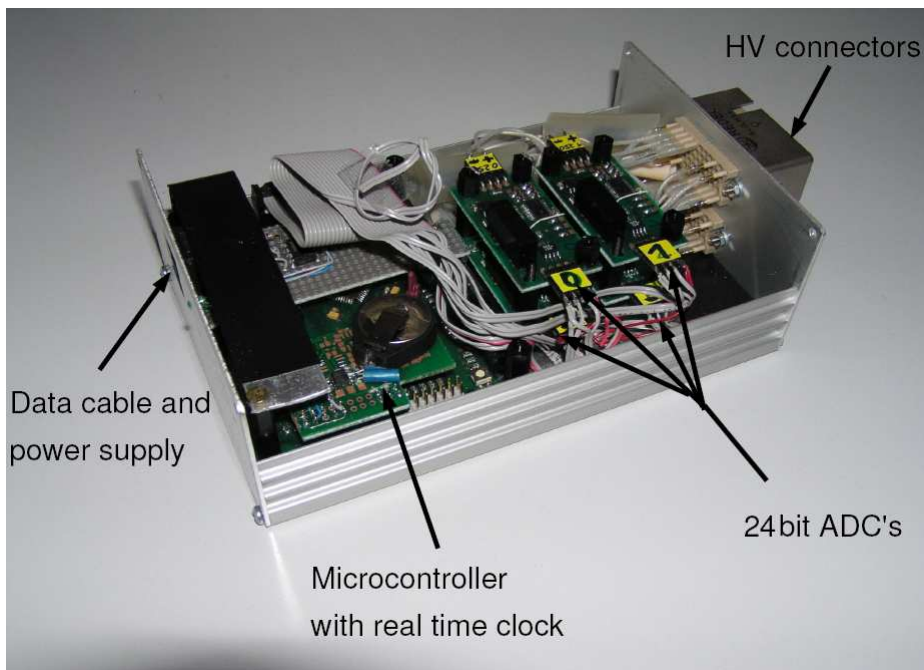
Figure 3. Device for the additional independent measurement of the HV current. The four 24 bit ADCs for the four HV current readout channels of the FCALchick are connected to a microcontroller to process their data and to add a timestamp from the real time clock to each measurement. The readout frequency is 10 Hz per channel and the resolution is 1.2 nA per bit.

2.4 Data taking

During test beam data-taking it was possible to move the cryostats horizontally, perpendicular to the beam line such that either the 250 μm side or the 100 μm side of the FCALchick could be centered on the beam. During the runs labelled as 230 and 240-244 the position of the FCALchick cryostat was adjusted such that the beam was centered to the 250 μm side. The cryostat position was kept constant, and the running conditions were stable. These runs are thus used for further analysis. Channel 3 of the 250 μm side of the FCALchick was not functioning during the April run and the corresponding ADC was therefore connected to channel 6 of the 100 μm side as indicated in figure 2.

As a reference for the beam intensity, the measurements of the calibrated ionisation chamber were used, providing one integrated measurement per spill. Periods with different beam positions relative to the FCALchick were analysed separately, because the particle flux through the calorimeter, and thus the HV current, depends on the calorimeter position relative to the beam while the beam intensity measured by the ionisation chamber is independent of the calorimeter position.

3 Analysis of the test beam data

3.1 Analysis of HV currents

The HV current was measured every 100 ms. However, the system was not synchronized with the beam trigger and no additional information was available on whether a measurement took place

Table 2. HV current thresholds for separating spill data from noise in units of nA. The low intensity run 230 is treated separately from the high intensity runs 240-244.

Run	Channel 0	Channel 1	Channel 2	Channel 6
230	470	100	400	80
240-244	600	150	460	70

within a spill or outside. For this reason it was necessary to separate the measurements of the HV current during a spill from those between two spills where dark current background and electronic noise dominates. This separation was done by requiring that measurements within a spill have to be at least three standard deviations above the noise level. All measured currents above the threshold were assigned to a spill, whereas all currents below the threshold were considered noise. The thresholds applied are summarised in table 2.

The differences in the thresholds from channel to channel are due to different dark currents and electronic noise in the corresponding channels. The individual channels of the HV power supplies showed different noise levels, whereas the dark currents have their origin in ground loops or leakage currents in the calorimeter. Slight changes of these conditions were also seen from run to run leading to the different thresholds between the low-intensity run 230 and the runs 240-244 with higher intensity.

The measurements obtained for one channel of one selected spill in run 230 are plotted in figure 4. For the data analysis the mean of the background measurements between the previous and the current spill was subtracted from each measurement within the spill.
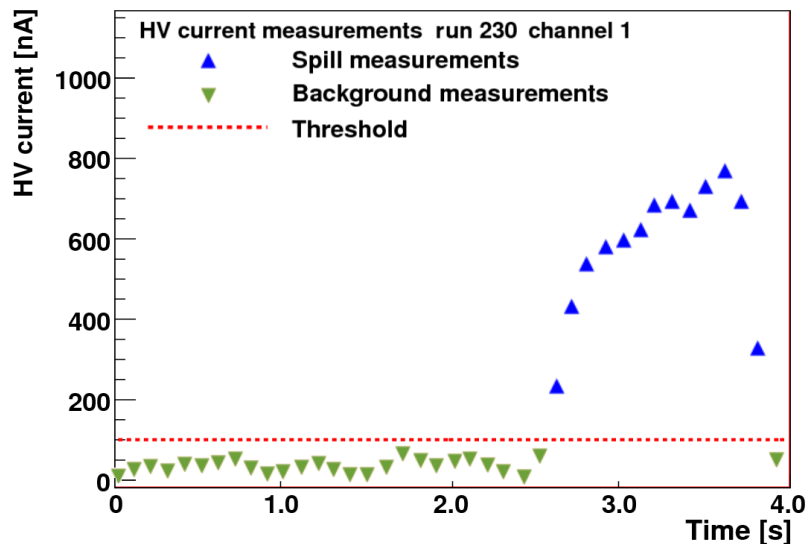
Figure 4. Measurements of the HV currents for one spill taken during run 230 for one of the four readout channels. Upward pointing triangles indicate measurements assigned to a spill. Downward pointing triangles correspond to background measurements between the spills. The horizontal line shows the threshold to separate the spills from background.

The integrated HV current for every spill was calculated for each channel independently as:

$$I = \sum_{i=1}^{n} (s_i - B) \cdot d. \tag{3.1}$$

Here, s_i are the measurements within the given spill, n is the number of such measurements, B is the mean of the background measured before the given spill and d is the time interval between two measurements within the spill. This integral is hence used for the comparison of the HV currents with the beam intensity measured by the ionisation chamber spill by spill.

The main contribution to the uncertainty on the integral is due to the electronics noise. It could hardly be calculated from the fluctuations within the spills because beam intensity variations would cause an additional contribution. Therefore this uncertainty was estimated from the fluctuations of the background measurements. Using the uncertainty on the mean of the background, $\triangle B$, with

$$\triangle B = \frac{1}{\sqrt{m \cdot (m-1)}} \sqrt{\sum_{i=1}^{m} (B - b_i)^2}, \tag{3.2}$$

the uncertainty on the integrated beam intensity is then given by:

$$\triangle I = \sqrt{[(n \cdot d \cdot \triangle B)^2 + n \cdot (d \cdot \triangle s_i)^2]} = n \cdot d \cdot \triangle B \cdot \sqrt{1 + \frac{m}{n}}, \tag{3.3}$$

where b_i are the background measurements before the given spill and m is the number of such measurements. The uncertainty on a single measurement, $\triangle s_i$, is estimated from the data in the time interval between spills as $\triangle s_i = \sqrt{m} \cdot \triangle B$.

The spills identified in the HV data stream were matched to the ionisation chamber measurements using a 3 s time window, much smaller than the 9.5 s interval between spills. The integral calculated from eq. 3.1 with the corresponding uncertainty calculated from eq. 3.3 are then compared to the beam intensity measurements of the ionisation chamber.

Very few cases were found where the beam intensity measured by the ionisation chamber was inconsistent with those from the scintillation counters, possibly due to readout instabilities. These data were removed from the subsequent analysis.

3.2 Beam position variations

The position of the FCALchick cryostat was kept constant during the runs 230 and 240-244, but small variations of the beam impact point could not be excluded. To investigate these variations, the integrated currents of the four channels were compared. A significant change of the ratio of currents between two channels would indicate a shift of the beam position. All six possible ratios were analysed: channels 0-1 and 2-6 for horizontal variations, channels 0-2 and 1-6 for vertical variations and channels 0-6 and 1-2 for the diagonal directions (see the channel layout in figure 2). Two ratios between the different channels are shown in figure 5, indicating a horizontal displacement in the left plot and a diagonal displacement in the right plot.

Two clearly separated peaks can be identified. Each of the two peaks corresponds to one of two run periods, period A containing runs 230, 240, and 241 and period B containing runs 242-244, with nearly constant beam position within each period. Because the exact profile of the proton
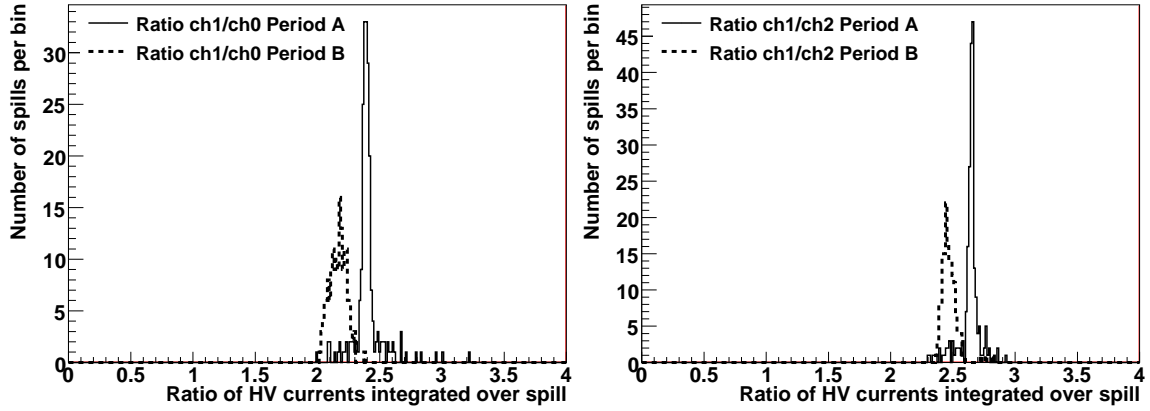
Figure 5. Ratios of HV currents between channel 1 and channel 0 in the left plot and channel 1 and channel 2 in the right plot for runs 230, 240-244. For each channel the integrated HV current over one spill is used to calculate the ratios.

beam after the primary absorber is poorly known, the difference in the HV current of the four channels for different beam positions cannot be easily predicted. Therefore the two data taking periods were analysed separately.

3.3 Investigation of non-linearities

To investigate possible non-linearities between the HV current and the beam intensity, a second order polynomial of the form

$$I = P_1 \cdot J + P_2 \cdot J^2, \tag{3.4}$$

was used to fit the data. Here, I is the HV current integrated over the spill in units of nC, and J is the beam intensity in units of $10^6 p$/spill, as measured by the ionisation chamber with the linear coefficient P_1, and the coefficient of the quadratic term, P_2. The non-linear fraction, N, of the HV current was calculated as:

$$N(J) = \frac{P_2}{P_1} \cdot J, \tag{3.5}$$

depending linearly on the beam intensity J.

A comparison of the HV current to the beam intensity measured by the ionisation chamber, both integrated over each spill, is shown in figure 6 together with the results of the fit for the two periods A and B. Also given in the middle plot of figure 6 is a magnified view of run 230 at lowest intensities. The fit is a combined fit of the channels 0, 1 and 2 which means it is applied to the HV current summed over these three channels in dependence on the beam intensity. These are the channels with 250 µm LAr gaps, whereas the fourth ADC was connected to channel 6 of the 100 µm side.

The parameters obtained in these fits for the two periods are summarised in table 3. The fit parameters in the lines labelled as "$\sum(0,1,2)$" were taken from the combined fit. From the calibration with activated aluminium foils it can be concluded that the relative precision of the beam intensity measurement by the ionisation chamber is better than 5% which is the accuracy of the calibration method. This is however only an upper bound on the uncertainty. Assigning a reduced

Table 3. Fit parameters of the non-linear fit for period A (runs 230, 240, 241) and period B (runs 242, 243, 244). The unit $10^6 p$/spill is used for the beam intensity to obtain the fit parameters. A scaling factor of 10^3 is applied in the last column in order to obtain the non-linear fraction at a beam intensity of $10^9 p$/spill which corresponds to the nominal LHC luminosity .

| Period	Channel	P_1	$P_2 \cdot 10^5$	χ^2(DoF)	$P_2/P_1 \cdot 10^6$	$N(J) \cdot 10^2$ $J = 10^9 \ p$/spill
A	0	2.39 ± 0.01	0.08 ± 0.17	326(217)	0.35 ± 0.70	0.03 ± 0.07
	1	5.64 ± 0.01	2.11 ± 0.25	277(217)	3.74 ± 0.45	0.37 ± 0.05
	2	2.17 ± 0.01	-0.14 ± 0.14	225(217)	-0.63 ± 0.64	0.06 ± 0.06
	6	3.29 ± 0.01	-0.53 ± 0.16	186(217)	-1.60 ± 0.48	0.16 ± 0.05
	$\sum(0,1,2)$	10.17 ± 0.02	2.69 ± 0.51	241(217)	2.64 ± 0.51	**0.26 ± 0.05**
B	0	3.31 ± 0.01	-19.0 ± 2.1	457(161)	-57.4 ± 6.6	5.74 ± 0.66
	1	6.69 ± 0.02	32.1 ± 4.6	189(161)	48.0 ± 7.1	4.80 ± 0.71
	2	2.89 ± 0.01	-15.4 ± 1.8	204(161)	-53.2 ± 6.3	5.32 ± 0.63
	6	2.14 ± 0.01	12.9 ± 1.6	206(161)	60.3 ± 7.6	6.03 ± 0.76
	$\sum(0,1,2)$	12.93 ± 0.05	-7.6 ± 8.1	126(161)	-5.9 ± 6.2	**0.59 ± 0.62**

uncertainty of 1.2% to the measurements of the ionisation chamber a much better behaviour of the χ^2 per degree of freedom of the fits was found. This value was used for obtaining the final result. The quadratic contribution of the term is given for $J = 10^9 \ p$/spill which corresponds to the nominal LHC luminosity of 10^{34} cm^{-2} s^{-1} (see table 1).

Using the summed current, the measured non-linear fraction is (0.26 ± 0.05) % for period A and (0.59 ± 0.65) % for period B at a beam intensity of $10^9 \ p$/spill. The reason for the larger uncertainty on the non-linear fraction in period B is due to the smaller beam intensity range up to $1.1 \cdot 10^9 \ p$/spill compared to a maximum of $5.5 \cdot 10^9 \ p$/spill for period A.
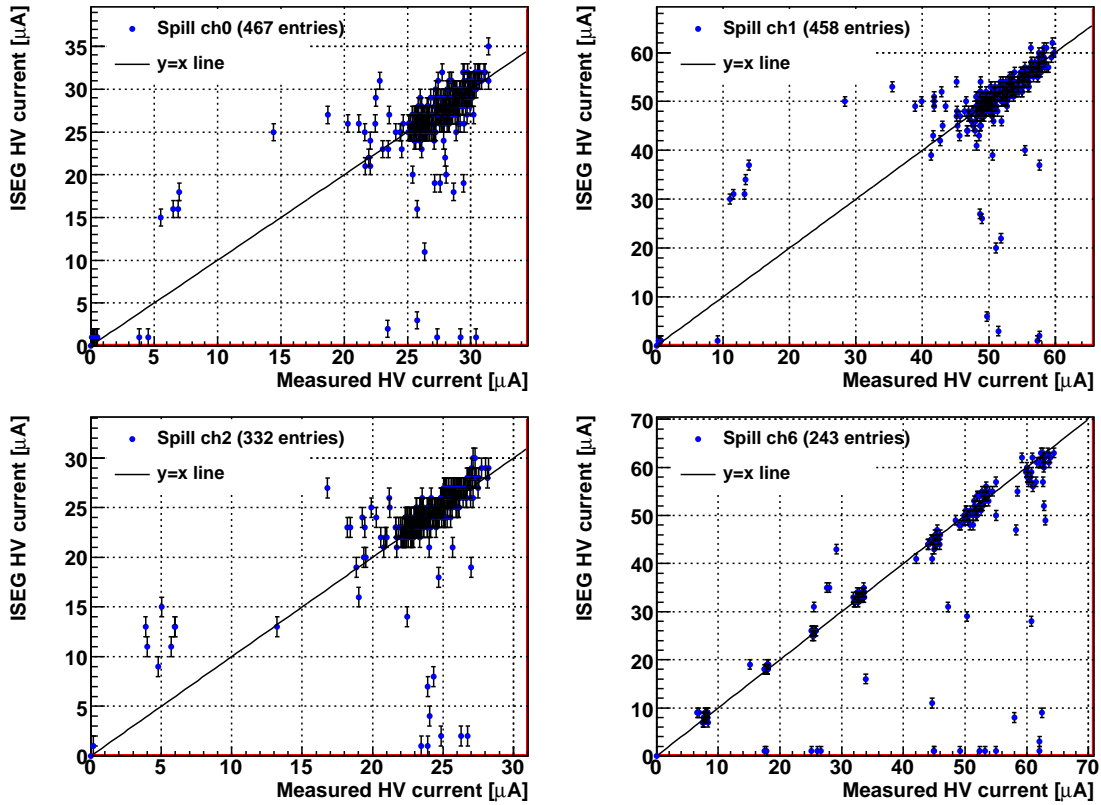
3.4 Comparison of HV currents measured externally with HV power supply currents

In ATLAS the measurement of the FCal HV currents will be performed directly by the ISEG HV power supplies [16]. To ensure that this method of measuring the relative luminosity can be used in ATLAS it has to be shown that the HV currents measured by the external measurement device and the ISEG internal measurement device are in agreement. One example for such a comparison is shown in figure 7. The integral of the current over the U-70 accelerator spill as measured by the external device was divided by the spill length. This value was compared to the ISEG measurements in the corresponding spill stored in the PVSS data archive [19]. As only one single measurement per spill with a precision of the timestamp of 1 s was available for the PVSS data stream, it is unknown where within the spill the measurement took place. The data points which are not in agreement with an ideal linear dependence are therefore due to measurements close to the start or end of the spill, where the intensity is varying strongly.

Since the two ammeters have different low pass filters the time constants to resolve the spill variation are not the same. These constants are 2.2 ms and 48.2 ms for the ISEG module and the external device, respectively. These deviations from linearity are well reproduced when simulating
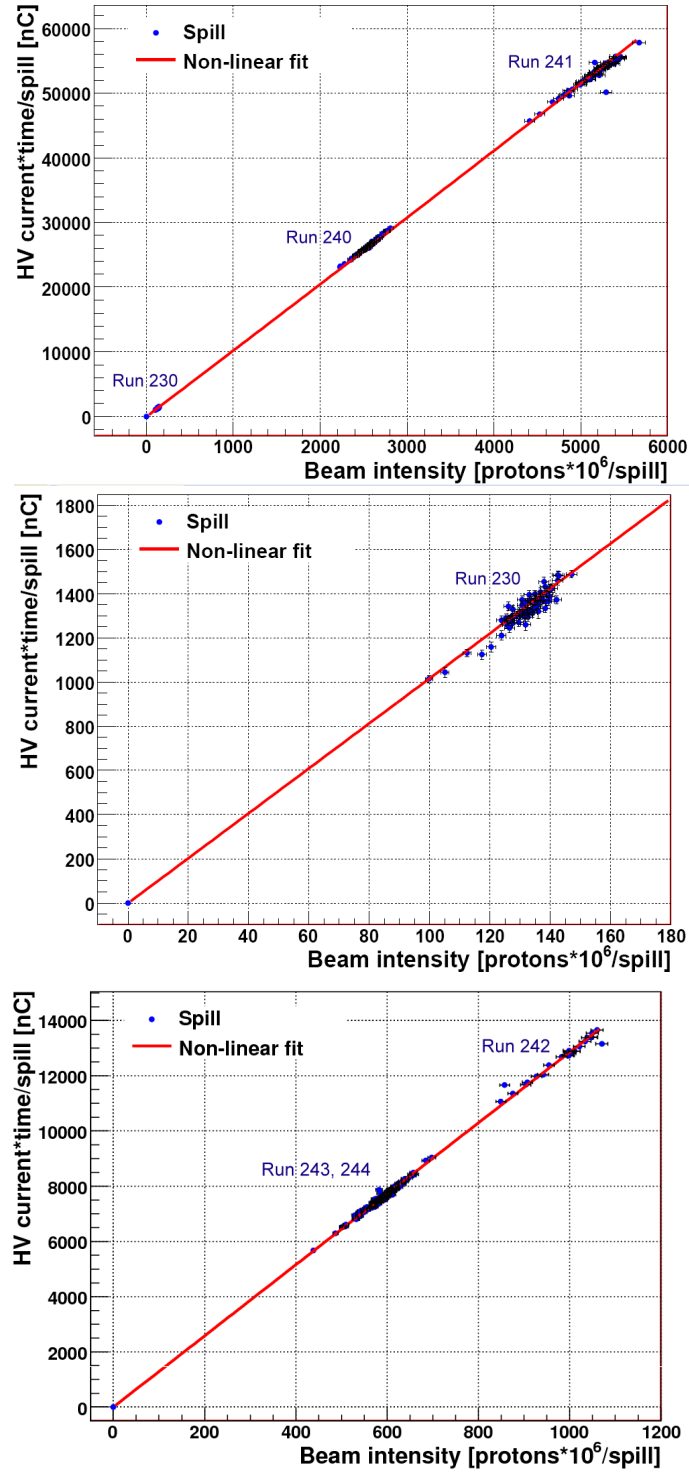
Figure 6. Measured HV current summed over the channels 0, 1, and 2 vs. beam intensity compared to a non-linear fit for period A (runs 230, 240, 241) in the top plot, a magnified view of run 230 in the middle plot, and period B (runs 242-244) in the bottom plot.

Figure 7. Comparison of the ISEG internal measurements of the HV current and the HV current measured by the external measurement device for runs 211-223 on a spill-by-spill basis.

the signal responses. When taking the different time constants into account, the measurements of both devices are in very good agreement. In conclusion, the ISEG HV module will be suitable for performing the measurements of the current, in particular when the ATLAS version of the module is used which provides a higher measurement precision with 20 bit ADCs instead of the 16 bit ones used for the Protvino test beam runs.

3.5 Results

The results of the run periods A and B are in very good agreement. They clearly show that the HV current measured by the FCal1 depends linearly on the beam intensity. Combining all data a non-linear fraction of less than 0.36 % at 95% confidence level was obtained. This applies to a beam intensity of $1 \cdot 10^9$ p/spill which corresponds to the nominal LHC luminosity of 10^{34} cm^{-2} s^{-1}.

The result for the channel with 100 μm gap is consistent with that from the 250 μm gap. This shows the robustness of the method against varying gap sizes and indicates the potential for using it during the sLHC phase as well.

3.6 Implications for the relative luminosity measurement in ATLAS

The differences between the fixed target experiment in Protvino and a collider experiment like ATLAS have to be taken into account when interpreting the test beam results for ATLAS. How-

ever, the proposed method is also applicable in ATLAS because the secondary particle flux is proportional to the beam intensity in a fixed target experiment and to the instantaneous luminosity in a collider experiment.

Furthermore, the differences between the ATLAS FCal1 and the FCALchick have to be considered. The main differences are the different proportions of both calorimeter modules. The tubes of the FCALchick are nine times shorter than that of the FCal1 in ATLAS and the FCALchick consists only of four channels with four tubes each as described in section 2. In addition, only one tube group of the FCALchick was connected to each HV supply channel instead of 64 tube groups in ATLAS [16]. Therefore it can be expected that the HV current per channel and that for the whole calorimeter will be much larger at the same particle flux in the ATLAS FCAL1 than for the FCALchick in the test beam. Thus statistical fluctuations per HV channel can be assumed to be further reduced.

The different beam structure in Protvino compared to that at the LHC will not influence the luminosity measurement using the FCal1 HV currents because the low pass filters will cause an averaging over many bunch crossings, resulting in a continuous DC current visible in the HV current readout. It is already seen that variations of the background current and noise between the different FCal channels are present in ATLAS and also variations in time are observed. Therefore, the selection of stable channels and investigations of thresholds to separate signal from background currents are important when applying the measurement to ATLAS.

3.7 Discussion of systematic uncertainties

Additional systematic effects (as discussed in [6]) may influence the measurements. Recombination of argon ions and electrons produced, as well as temperature effects can be assumed as being already included in the test beam result. Furthermore, the operating conditions of the liquid argon of the calorimeter (temperature of about 89 K, purity of about 2 ppm) during the Protvino April 2008 run were nearly the same as expected in ATLAS. The FCal1 HV currents caused by detector activation could be higher than that in Protvino because of the larger detector volume. But these currents can be neglected with respect to those due to primary interactions in ATLAS [6].

Therefore, only the systematic effects due to a displacement of the mean interaction point and due to lost beam particles reaching the FCal1 could possibly deteriorate the linear response of the FCal1 HV currents in ATLAS significantly. The effect of lost beam particles (e.g. due to beam-gas interactions) is however expected to be negligible because of the forward shielding installed in ATLAS [6].

The variations of the HV current caused by a displacement of the mean interaction point of 1 cm along the beam axis is expected to be less than 0.2 % in each FCal1 module. This can be further reduced to 0.1 % by summing over the currents of the FCal1 modules on both sides of the ATLAS detector [6]. A possible lateral displacement of the mean interaction point would introduce a significant transverse asymmetry in the pattern of currents drawn from the HV power supplies. However, as long as such a displacement is constant in time it will not influence the linearity of the relative luminosity measurement.

4 Summary and conclusion

In this paper an alternative method for a relative luminosity measurement at the LHC using the readout of the high voltage return current in the forward section of the liquid-argon calorimeter of ATLAS was discussed. The analysis of test beam data taken at the U-70 proton accelerator in Protvino using a prototype of the forward calorimeter was described and the proposed method was verified.

A linear relation between the HV current measured with the FCALchick and the beam intensity was found with a non-linear fraction of less than 0.36 % (95% CL) at a beam intensity of $1 \cdot 10^9$ p/spill, corresponding to the nominal ATLAS luminosity of 10^{34} cm^{-2} s^{-1}. The most important systematic uncertainty of approximately 0.1 % is expected to be caused by variations of the mean interaction point in ATLAS. Taking statistical and systematic uncertainties into account, a precision of better than 0.5 % will be feasible for ATLAS.

References

[1] The ATLAS Collaboration, G. Aad et al., *The ATLAS experiment at the CERN Large Hadron Collider*, 2008 *JINST* **3** S08003.

[2] L. Evans, Ph. Bryant, *LHC machine*, 2008 *JINST* **3** S08001.

[3] ATLAS collaboration, *ATLAS forward detectors for measurement of elastic scattering and luminosity*, CERN-LHCC-2008-04.

[4] S. Ask et al., *Luminosity measurement at ATLAS-development, construction and test of scintillating fibre prototype detectors*, *Nucl. Instrum. Meth.* **A 568** (2006) 588;
F. Anghinolfi et al., *Hadron beam test of a scintillating fibre tracker system for elastic scattering and luminosity measurement in ATLAS*, 2007 *JINST* **2** P07004.

[5] The ATLAS Collaboration, S. Ask, *Simulation of luminosity monitoring in ATLAS*, ATL-LUM-PUB-2006-001 (2006).

[6] The ATLAS Collaboration, W. Bonivento, *Online luminosity monitoring with liquid Argon calorimeters at ATLAS and D*0, ATL-LARG-2001-001 (2001).

[7] T. Sjostrand, S. Mrenna and P. Skands, *PYTHIA 6.4 physics and manual*, *JHEP* **05** (2006) 026.

[8] R. Engel, *Photoproduction within the two-component dual parton model: amplitudes and cross sections*, Z. Phys. C 66 203, 1995.

[9] S. Ivanov et al., *Accelerator complex U70 of IHEP-Protvino: status and upgrade plans*, in the proceedings of *RuPAC* 2008, September 28–October 3, Zvenigorod, Russia (2008), online at http://accelconf.web.cern.ch/accelconf/r08/papers/TUBAU01.pdf.

[10] J. Rutherfoord, *Signal degradation due to charge buildup in noble liquid ionization calorimeters*, Nucl. Instrum. Meth. **A 482** (2002) 156.

[11] HiLum ATLAS Endcap collaboration, *Liquid argon calorimeter performance at high rates*, to be published.

[12] P. Schacht, *ATLAS liquid argon endcap calorimeter R&D for sLHC*, in the proceedings of the 11th *International Conference on Advanced Technology and Particle Physics (ICATPP) Conference*, October 5–9, Villa-Olmo, Italy (2009), World Scientific, Singapore (2009) [ATL-LARG-PROC-2009-013].

[13] Yu.A. Tikhonov for the ATLAS Liquid Argon HiLum group, *Operation of the ATLAS end-cap calorimeters at sLHC luminosities: An experimental study*, in the proceedings of the 11th *Pisa Meeting onA dvanced Detectors*, May 24–30, La Biodola, Isola d'Elba, Italy (2009), to be published in *Nucl. Instrum. Meth.*.

[14] J.-P. Koutchouk and F. Zimmermann, *LHC upgrade scenarios*, sLHC-Project-Report-0013 (2009).

[15] A.G. Afonin et al., *High-efficiency beam extraction and collimation using channeling in very short bent crystals*, Phys. Rev. Lett. **87** (2001) 094802.

[16] A. Artamonov et al., *The ATLAS forward calorimeters*, 2008 *JINST* **3** P02010.

[17] S. Agostinelli et al., *Geant4 — A simulation toolkit*, Nucl. Instrum. Meth. **A 506** (2003) 250.

[18] ISEG company, Rossendorf near Dresden, Germany, online at http://www.iseg-hv.com.

[19] ETM professional control, Laatzen, Germany, online at http://www.etm.at/index.asp?id=2.